京 都 大 学 防 災 研 究 所 年 報　第47号 B　平成16年4月
Annuals of Disas. Prev. Res. Inst., Kyoto Univ., No. 47 B, 2004

A model for flood inundation analysis in urban area: verification and application

Nguyen Tat THANG*, Kazuya INOUE, Keiichi TODA, and Kenji KAWAIKE**

*International Student, Faculty of Engineering, Kyoto University
**Nagasaki University

Synopsis

A mathematical model based on unstructured meshes for analyzing 2-D flood inundation is presented. The model is first verified by using experiment data provided by Ujigawa Hydraulic Laboratory Group, DPRI, Kyoto University. Additional verification analysis is carried out by using rough measured data of a flood inundation caused by heavy rainfall in Hanoi city of Vietnam in 2001. In general, the verification results are acceptable. The model is then applied to analyze 2-D flood inundation in the Hanoi central area. The model application includes the following analyses: an assumed exceptionally heavy rainfall analysis and an assumed dike break analysis. The application results give an overview of flood disasters if they happen to the city. These results show that the model could be a useful tool for the city flood control and for prediction of flood inundation process in any areas of interest.

Keywords: Unstructured meshes, flood inundation analysis, model verification, Hanoi, heavy rainfall, dike break, Red River

1. Introduction

Numerical simulations for 2-D flood inundation have been much developed. These simulations are important in studying flood inundation process in flood prone areas including: plain areas, residential areas or urban areas etc. They are also significant in management works and decision support systems of any area. The numerical methods which are widely used in flood inundation simulations are: traditionally, the finite difference method (FDM); secondly, the finite element method (FEM) and presently, the finite volume method (FVM) etc. In addition, some modified schemes based on these methods have been successfully implemented. Among these schemes, the one developed by Kawaike et al. (2000) based on unstructured meshes and the finite volume method is efficient one in studying flood inundation process in urban areas. Thanks to the flexibility of unstructured meshes and a simple mathematical approach, the scheme is suitable for city areas where the topography is often complicated and the flood inundation time is usually not too long. In order to develop a model for urban flood inundation analysis, the Kawaike's method is applied in this study. The model is verified using experiment data of a large scale experiment model for flood inundation study in Kyoto city area (Ishigaki et at., 2003). The data was provided by Ujigawa hydraulic laboratory group, DPRI, Kyoto University. The model application includes some flood inundation analyses for the Hanoi capital city of Vietnam. In the past, this area ever underwent real risks of Red River dike break during flood seasons (Tinh, 2001). Besides 2-D flood inundation analysis for this area is a relatively new topic. Recently, most of the flood analyses for this area have been concentrated on 1-D flood simulations in the Red River system. In rainy seasons, some parts of the city are usually flooded by heavy rainfalls. Moreover some very big hydropower dams, such as the dam of Hoa Binh (completed) and the dam of Son La (under construction), are located in the upstream area of the Red River. As a result, there appears more and more potential of dangerous dike breaks in the downstream areas when sudden extraordinarily big floods or

upstream hydropower dam failures occur. In such cases, severe floods are not confined in the approximated 1-D river channels, but rather in 2-D inundation areas (Tinh, 2001). Therefore the application focuses on prediction and assessment of flood inundation processes caused by assumed extraordinarily heavy rainfall or river dike break in the area. The study aims to develop a tool to assist the city water drainage and management work.

2. Numerical technique

Numerical solutions for 2-D overland flood flows have been developed by Iwasa and Inoue (1982) and by Inoue et al. (1994) using the finite difference scheme based on Cartesian meshes; Kawaike et al. (2000) applied the finite difference scheme based on unstructured meshes and the finite volume method. These methods were successfully applied to solve numerically the system of the two-dimensional shallow water equations for flood inundation simulation. The method based on unstructured meshes has advantages to describe complicated areas more exactly and it is applied in this study.

2.1 Basic equations for unsteady 2-D water flow

2-D unsteady flood flows with considerations of rainfall intensity and drainage capacity can be described by the system of shallow water equations, including:

Continuity equation:

$$\frac{\partial h}{\partial t}+\frac{\partial M}{\partial x}+\frac{\partial N}{\partial y}=q_{rain}-q_{drain} \tag{1}$$

Momentum equations:

$$\frac{\partial M}{\partial t}+\frac{\partial (uM)}{\partial x}+\frac{\partial (vM)}{\partial y}=-gh\frac{\partial H}{\partial x}-\frac{gn^2M\sqrt{u^2+v^2}}{h^{4/3}} \tag{2}$$

$$\frac{\partial N}{\partial t}+\frac{\partial (uN)}{\partial x}+\frac{\partial (vN)}{\partial y}=-gh\frac{\partial H}{\partial y}-\frac{gn^2N\sqrt{u^2+v^2}}{h^{4/3}} \tag{3}$$

where t is time; u and v are x and y components of mean velocity; h is water depth; $M=uh$ and $N=vh$; $H=h+z_b$ where z_b is bed elevation from the reference datum; g is the gravitational acceleration; n is the Manning roughness coefficient; q_{rain} is rainfall intensity; q_{drain} is drainage capacity which is approximated to be the depth of water drained away per unit time through drainage and sewerage system.

2.2 Solution approach using unstructured meshes

The method uses the finite difference technique based on unstructured meshes (Kawaike et al., 2000). The study area is divided into convex polygons having arbitrary numbers of sides (Fig.1). Locations of M , N and h variables, discrete variables in the difference equations, are chosen at the center of each side and at the centroid of each mesh, respectively (Fig.1). As shown below in Fig.1, *A* and *B* are meshes used to determine *M, N, u* and *v* of the side *L*; *C* is an individual mesh used to determine *h* of the mesh *C*.

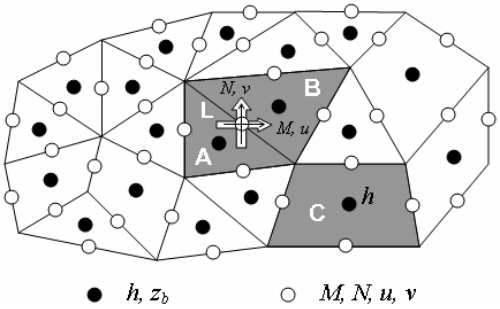

Fig.1 Unstructured meshes and locations of variables

As shown in Fig.1, h can be determined by using only mesh C . Generally we can suppose a control volume for the continuity equation as shown in Fig.2 and the finite difference form for the continuity equation, Eq.1, is:

$$\frac{h^{n+3}-h^{n+1}}{2\Delta t}+\frac{1}{A}\sum_{l=1}^{m}\left(M_l^{n+2}(\Delta y)_l-N_l^{n+2}(\Delta x)_l\right)=q_{rain}-q_{drain} \tag{4}$$

where *m* is number of sides of the polygon (control volume); *A* is area of the polygon (control volume); M_l , N_l are *x* and *y* components of the discharge flux on the side *l* of the control volume polygon; $(\Delta x)_l$ and $(\Delta y)_l$ are the differences of the x and y coordinates at both ends of the side l , respectively; *n* is the time step increment.

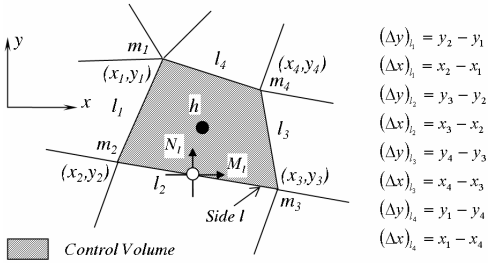

Fig.2 Control volume for continuity equation

On the other hand, M , N are located on a side, e.g. side L . The determination of M , N needs both adjacent meshes A and B of the side L (Fig.1). Generally the control volume for the momentum equation is selected as shown in Fig.3 and the finite difference forms for Eq.2 and Eq.3 are:

$$\frac{M_L^{n+2}-M_L^n}{2\Delta t}+m1+m2=-g\tilde{h}_L^{n+1}(\nabla H)_x-gn^2\frac{\frac{M_L^{n+2}+M_L^n}{2}\sqrt{\left(u_L^n\right)^2+\left(v_L^n\right)^2}}{\left(\tilde{h}_L^{n+1}\right)^{4/3}} \tag{5}$$

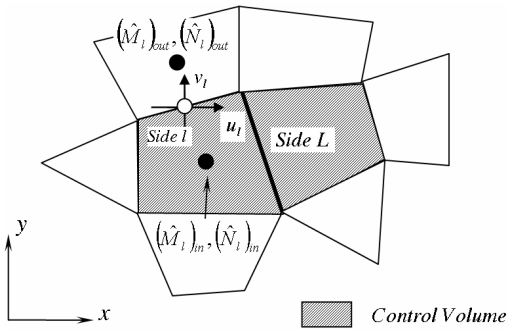

Fig.3 Control volume for momentum equations

$$\frac{N_L^{n+2}-N_L^n}{2\Delta t}+n1+n2=-g\tilde{h}_L^{n+1}(\nabla H)_y - gn^2\frac{\frac{N_L^{n+2}+N_L^n}{2}\sqrt{(u_L^n)^2+(v_L^n)^2}}{(\tilde{h}_L^{n+1})^{4/3}} \quad (6)$$

where n is the time step increment; M_L and N_L are discharge flux components to be determined on the side L of the polygon; the terms *m1+m2* and *n1+n2* will be described later; $(\nabla H)_x$ and $(\nabla H)_y$ are x- and y- components of the gradient of water surface H between mesh *i* and mesh *j* (Fig.4) and they are expressed respectively as follows:

$$(\nabla H)_x=\frac{H_j^{n+1}-H_i^{n+1}}{DL}\frac{x_j-x_i}{DL} \quad (7)$$

$$(\nabla H)_y=\frac{H_j^{n+1}-H_i^{n+1}}{DL}\frac{y_j-y_i}{DL} \quad (8)$$

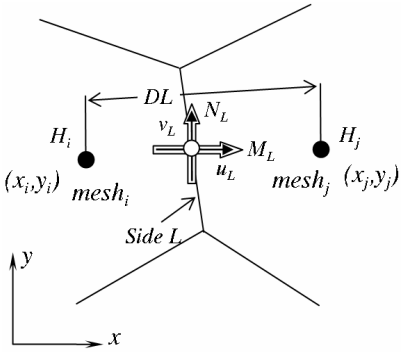

Fig.4 Variables used in the calculation of momentum

where H_i and H_j are water levels of the mesh *i* and *j*, respectively; (x_i,y_i) and (x_j,y_j) are coordinates of the centroid of the mesh *i* and *j*, respectively; *DL* is distance between the centroids of the mesh *i* and *j*; and $\tilde{h}_L$ is the interpolated water depth on the side L and it is given by:

$$\tilde{h}=\left(\frac{h_i}{d_i}+\frac{h_j}{d_j}\right)\Big/\left(\frac{1}{d_i}+\frac{1}{d_j}\right) \quad (9)$$

where h_i and h_j are water depth of the mesh *i* and mesh *j*, respectively; d_i and d_j are distances between midpoint of the side *L* and the centroids of the mesh *i* and *j*, respectively (Fig.5).

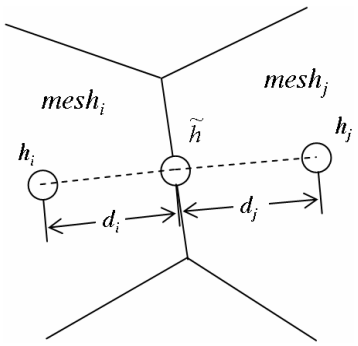

Fig.5 Interpolation of flow depth

In Eq.5 and Eq.6, u_L^n is x component of the flow velocity and it is defined as $u_L^n=M_L^n/\tilde{h}_L^{n+1}$; and v_L^n is y component of the flow velocity and it is defined as $v_L^n=N_L^n/\tilde{h}_L^{n+1}$.

Fig.3 shows the control volume for the convection terms *m1+m2* and *n1+n2* of the finite difference forms of the momentum equations. These terms are expressed by:

$$m1+m2=\frac{1}{A_{CV}}\sum_{l=1}^{m'}\left\{u_l^n\hat{M}_l^n(\Delta y)_l-v_l^n\hat{M}_l^n(\Delta x)_l\right\} \quad (10)$$

$$n1+n2=\frac{1}{A_{CV}}\sum_{l=1}^{m'}\left\{u_l^n\hat{N}_l^n(\Delta y)_l-v_l^n\hat{N}_l^n(\Delta x)_l\right\} \quad (11)$$

where A_{CV} is the area of the control volume shown in Fig.3; *m'* is the number of sides of the polygon as a control volume; u_l and v_l are x and y components of the flow velocities defined on the midpoint of the side l of the control volume polygon; $\hat{M}$ and $\hat{N}$ are x and y components of the discharge flux defined on the centroid of the mesh, respectively and they are given as follows:

$$\hat{M}=\left(\frac{M_1}{d_1}+\cdots+\frac{M_m}{d_m}\right)\Big/\left(\frac{1}{d_1}+\cdots+\frac{1}{d_m}\right) \quad (12)$$

$$\hat{N}=\left(\frac{N_1}{d_1}+\cdots+\frac{N_m}{d_m}\right)\Big/\left(\frac{1}{d_1}+\cdots+\frac{1}{d_m}\right) \quad (13)$$

where $M_1, M_2, \ldots, M_m, N_1, N_2, \ldots, N_m$ are discharge fluxes as shown in Fig.6. and $d_1, d_2, \ldots, d_m$ are distances between each midpoint of the sides and the centroid of the polygon.

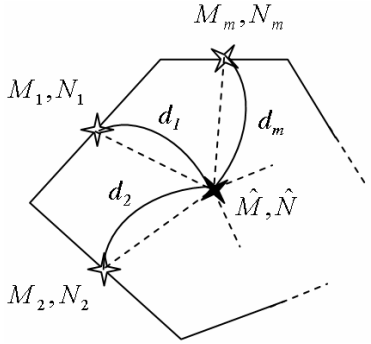

Fig.6 Interpolation of discharge flux

In Eq.10 and Eq.11, $\hat{M}_l^n$ and $\hat{N}_l^n$ are evaluated as follows:

For $u_l^n \hat{M}_l^n$, $u_l^n \hat{N}_l^n$:

$$\text{If } u_l^n (\Delta y)_l \geq 0 \text{ then } \begin{cases} \hat{M}_l^n = \left(\hat{M}_l^n\right)_{in} \\ \hat{N}_l^n = \left(\hat{N}_l^n\right)_{in} \end{cases} \quad (14)$$

$$\text{If } u_l^n (\Delta y)_l < 0 \text{ then } \begin{cases} \hat{M}_l^n = \left(\hat{M}_l^n\right)_{out} \\ \hat{N}_l^n = \left(\hat{N}_l^n\right)_{out} \end{cases} \quad (15)$$

For $v_l^n \hat{M}_l^n$, $v_l^n \hat{N}_l^n$:

$$\text{If } v_l^n (\Delta x)_l \geq 0 \text{ then } \begin{cases} \hat{M}_l^n = \left(\hat{M}_l^n\right)_{out} \\ \hat{N}_l^n = \left(\hat{N}_l^n\right)_{out} \end{cases} \quad (16)$$

$$\text{If } v_l^n (\Delta x)_l < 0 \text{ then } \begin{cases} \hat{M}_l^n = \left(\hat{M}_l^n\right)_{in} \\ \hat{N}_l^n = \left(\hat{N}_l^n\right)_{in} \end{cases} \quad (17)$$

where $\left(\hat{M}_l^n\right)_{in}$, $\left(\hat{M}_l^n\right)_{out}$, $\left(\hat{N}_l^n\right)_{in}$, $\left(\hat{N}_l^n\right)_{out}$ are the discharge fluxes as shown in Fig.6.

2.3 Boundary and initial conditions

The boundary conditions include the followings: dike-break, high wall and free overland flow conditions. As for the dike-break condition, the discharge fluxes of sides of meshes at the break point are calculated by using the known discharge hydrograph of break point. The high wall condition means that, at the physical boundaries, there is no flow flux through these boundaries and the flux is set to be zero. As for the free overland flow condition, the discharge fluxes, at those boundaries where flux could exist, are calculated by using drop type or step down flow formula:

$$M(N) = (2/3)^{3/2} h\sqrt{gh} \quad (18)$$

where h is water depth and g is gravitational acceleration.

3. Model verification

The model is verified by using experiment data provided by Ujigawa Hydraulic Laboratory Group, DPRI, Kyoto University. The scale of the hydraulic-experiment model is 1/100. The experiment models flood inundations in complicated area of Kyoto city.

3.1 Experiment model (Ishigaki et al., 2003)

The site of the experiment model (GS model site) is chosen as shown in Fig.7(a). This site is adjacent to Kamo river and highly urbanized with many buildings on the land surface and complicated structures in the underground space. In Fig.7(a) US model site is the site for the experiment of an Underground Space model (US model). This experiment is not studied here. GS model site, which covers the US model site, is the site for the experiment of the Ground Surface model. The results of this experiment model are used here. The GS model site covers a rectangular of 1km x 2km. The site of the experiment model is a 10m x 20m rectangle.

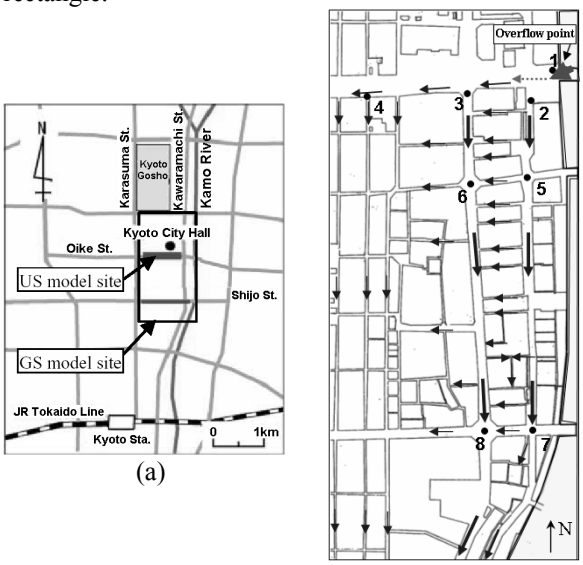

Fig.7 (a) The site of experiment model; (b) Water depth measurement points

The experiment includes two cases: without the underground (not consider underground space so there is no water flows into the underground) and with the underground (consider underground space so water is allowed to flow into the underground through some entrances). Fig.7(b) shows positions numbered from 1 to 8 where water depth is measured in both of the experiments.

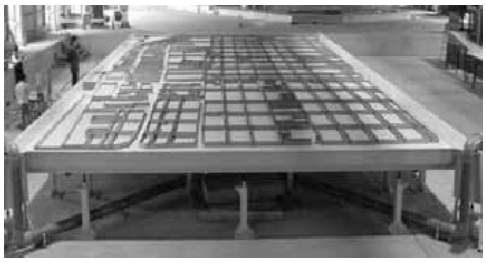

Fig.8 The experiment model

Fig.9 shows positions where outflow water discharges are measured. From number 1 to number 29 and from number 41 to number 59 are positions where water flows into the underground through some entrances in the Oike street and in the Shijo street, respectively. These discharges are measured in the experiment which considers the underground space. From number 61 to number 73 are positions where water flows out from the experiment area through streets.

The Manning roughness coefficient of the experiment is determined to be 0.01. Actually in the simulations, the value of Manning roughness coefficient is selected to be 0.014 for the whole area

except at meshes of intersections. At the intersections, the Manning roughness coefficient is chosen to be 0.02. This is due to the assumption that there would be energy loss or turbulent phenomena which happen in the experiment at the intersections or along streets.

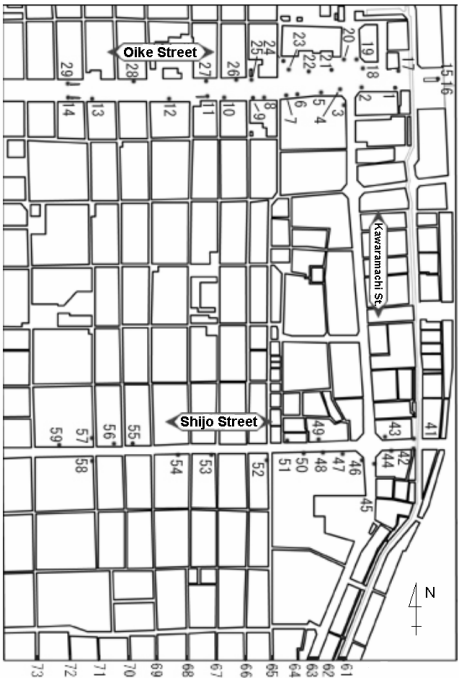

Fig.9 Discharge measurement points

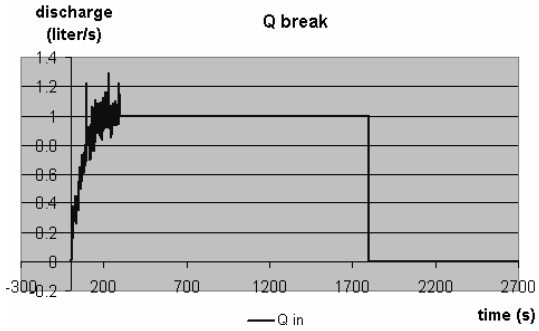

Fig.10 Discharge of the overflow

3.2 Numerical simulation

The experiment area is divided into 4996 unstructured meshes. The meshes of streets are very fine but shape of meshes of building blocks is kept almost the same as original shape of these blocks (Fig.11).

Ground elevation of street meshes is determined using information of the experiment model. Ground elevation of building blocks are assigned a high value, say 5.0 m, to prevent water invades into these meshes during the simulation since water is not allowed to flow into building blocks in both cases (with and without underground space) of the experiment.

Boundary conditions of the numerical simulation include the followings: the condition of the overflow point; the conditions of outflow number 61 to number 73 in the Fig.9; other boundaries are assumed high wall boundaries because, in the experiments, there is no water flows through these boundaries. For the first two boundary conditions the step down formula is assumed to calculate flux discharges of the boundary sides. At high wall boundaries flux discharges are set to be zero. At the entrances into the underground, the step down formula is also assumed. According to the experiment, a dry initial condition is used in the simulations.

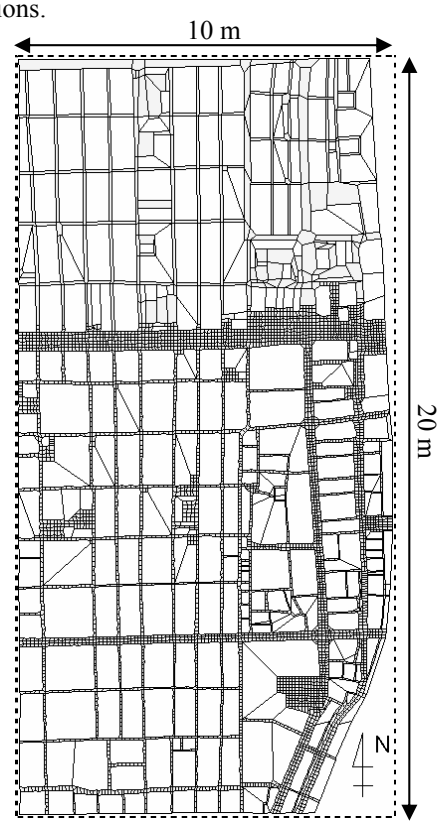

Fig.11 The computation meshes

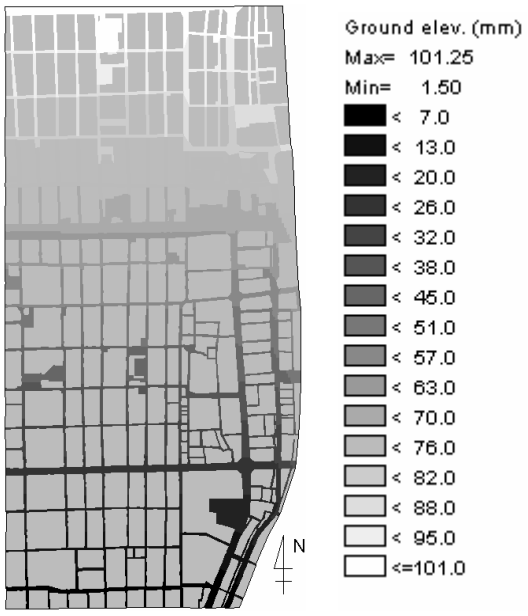

Fig.12 Elevation of the experiment area

3.3 Computed results and comparisons

The numerical simulations are carried out in both cases: without the underground and with the underground. The time step of both two cases is 0.05 second.

(1) Without the underground

In general, the invasion process of overflow water into the area simulated by the numerical model shows the same behavior with that of the experiment model. This is presented more detailed by the comparisons between computed water depths and measured ones at some points in the area (from Fig.14 to Fig.16). Fig.13 shows computed water depth in the whole area at an individual time (after 3 minutes).

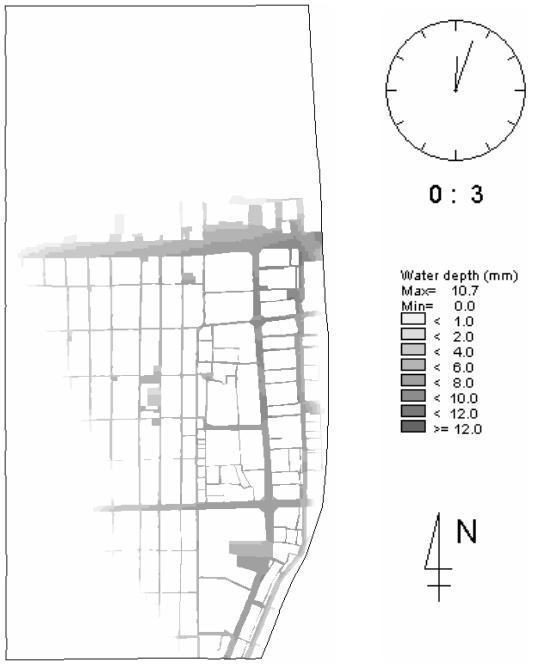

Fig.13 Computed water depth

The comparison between computed water depths and measured ones at eight points in Fig.7(b) shows that the percentage of the absolute error is almost within 20%. Computed water depths and measured ones at some selected points are shown in from Fig.14 to Fig.16.

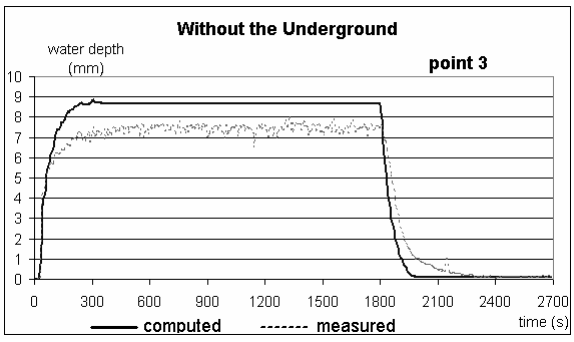

Fig.14 Comparison between the computed water depth and the measured one at point number 3

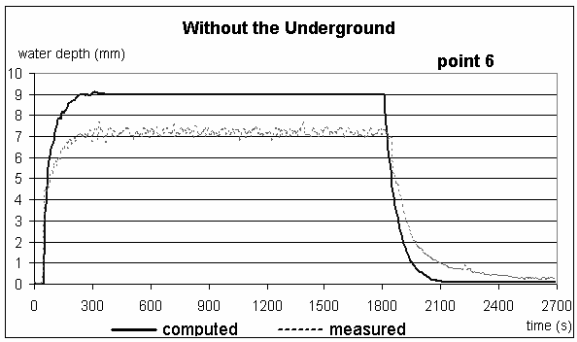

Fig.15 Comparison between the computed water depth and the measured one at point number 6

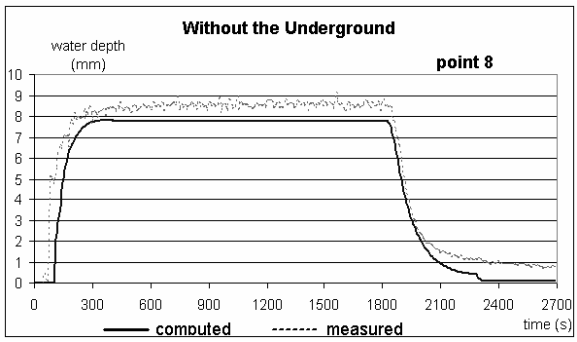

Fig.16 Comparison between the computed water depth and the measured one at point number 8

Those points, point No.3, 6 and 8, are located in the three main streets of this area: Kawaramachi, Shijo and Oike streets. Since a big amount of water flows along those streets, above points should be much cared about in the comparisons.

(2) With the underground

Fig.17 shows computed water depth in the whole area after 3 minutes.

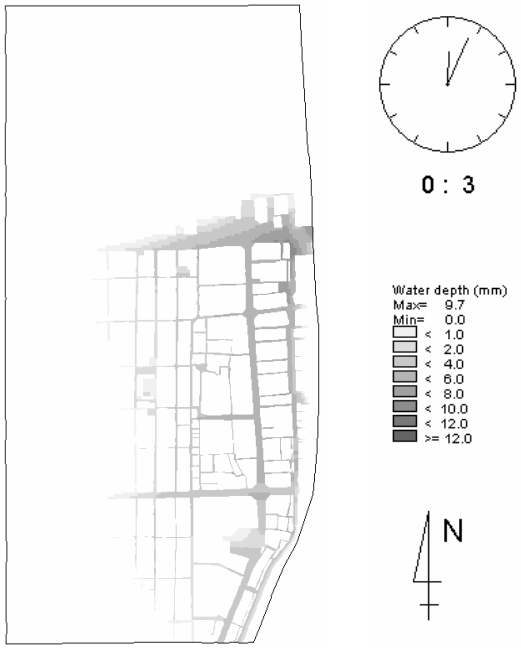

Fig.17 Overall water depth after 5 minutes

Similarly same behavior, as the previous simulation, of inundation process is obtained in this case. The comparison results also show that the errors between computed water depth and measured ones are within 20% except at point number 4. The computed discharge at this point is about 40% lower than measured one. This could be due to the fact that there are many entrances into underground located along the Oike street and the modeling of these entrances would not be exact enough. Therefore in the simulation, much water would go into the underground and it makes water depth at the point 4 lower. Computed water depths and measured ones at points number 3, 6 and 8 are shown below. In general, the computed results are acceptable.

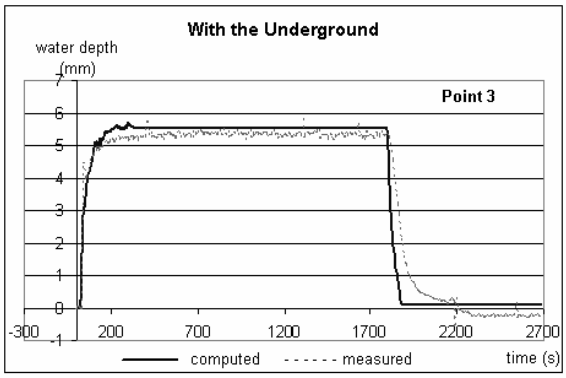

Fig.18 Comparison between the computed water depth and the measured one at point number 3

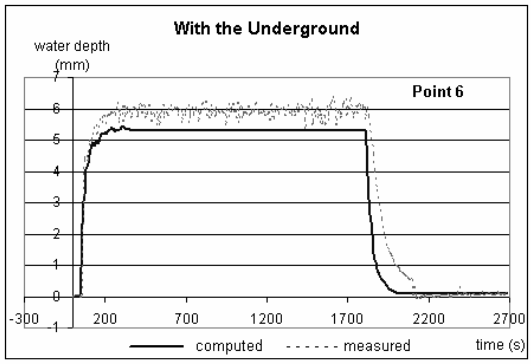

Fig.19 Comparison between the computed water depth and the measured one at point number 6

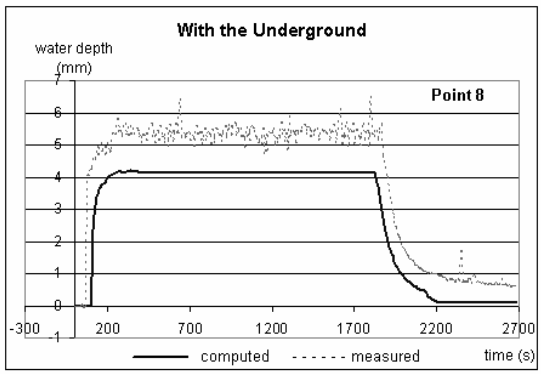

Fig.20 Comparison between the computed water depth and the measured one at point number 8

3.4 Discussion

The comparisons results at some points are quite good but not so good at some other points. In the case with the underground, the comparisons between the computed water depth and the measured one at point number 4 is rather bad. There would be some reasons that need to be much further studied about, such as:

- The distribution of the value of Manning roughness coefficient in the simulation area: this value might not be the same everywhere in the whole area.
- A proper modeling of discharge vector direction and distribution along overflow sides should be much cared.
- The turbulent problem: the experiment model includes many building blocks with sharp corners. They are believed discontinuity positions in the topography of the simulation area and there must be turbulent flows at these positions.
- The step down formula is applied at entrances to the underground. The application of this formula and value of coefficients in this formula should be much studied about when it is applied in this situation.
- The description of entrances in the computation meshes is not so exact because they are too small.
- Some efforts have been made to calibrate the flow discharges and to compare between computed discharges and measured ones at the points in Fig.9 but the results were not so good. As mentioned above, this could be due to the inexactness of the modeling of entrances into the underground and of the using of drop type formula. Another way of simulations is that ones could use these measured discharges as boundary conditions. This could be much further study about.

4. Model application

4.1 Description of the study area

The model is applied to the Hanoi central area located in the Red River delta (Fig.21). The Red River, flowing to the South East, is quite a big river with an average discharge about 10000 m^3/s in flood seasons (Fig.38). A dike system is located along both sides of the river. Over the centuries, the dike system has been gradually constructed and strengthened to protect cultivated land along both sides of the river (Tinh, 2001).

(1) Characteristics of the area

The city central area, including the government office areas, the shopping and traditional areas, is shown in Fig.22. The Red River, located on the North East side of the city, flows to the South East. There are some small lakes and rivers inside the area (Fig.25).

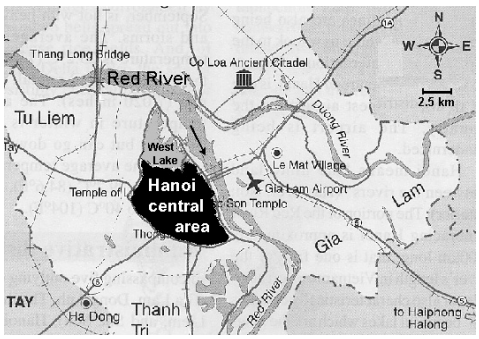

Fig.21 Location of the study area

The typical trend of the ground elevation in this area is the inclination in the South-West direction. Especially, the difference between the city ground elevation and the bed elevation of the Red River is not so significant; this is shown in Fig.23 for one cross section C1-C2 in Fig.22. During Red River floods, the water level of the Red River is usually higher than the city elevation (Fig.24).

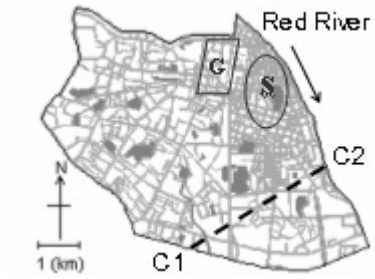

Fig.22 Major areas in the city (G: government offices area, S: shopping and traditional area)

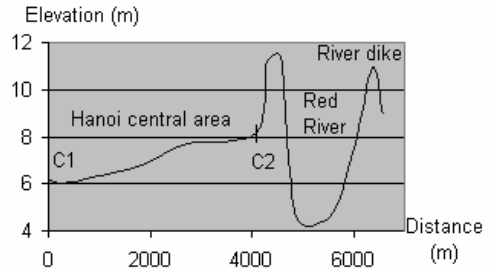

Fig.23 Cross section C1-C2 and its part in the Red River

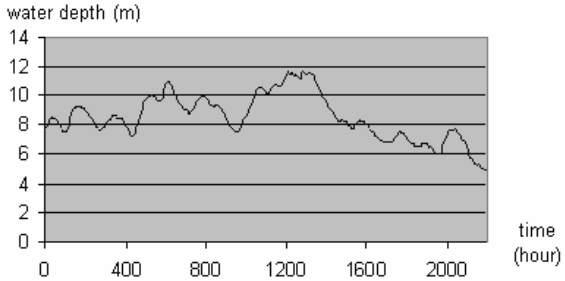

Fig.24 The observed water depth at Hanoi Station in Aug. 1996

(2) Flood disasters caused by heavy rainfalls

In rainy seasons, serious flood inundations caused by heavy rainfalls are quite common in the city (Photo 1). Especially, in the rainy season in 2001, an exceptional recorded rainfall of total 307 mm, which first happened in the past 17 years since 1984, brought widespread inundation to the city for hours.


Photo 1 A flood inundation caused by a heavy rainfall in the city

(3) Potential of river dike breaks

There exists a real potential of dike breaks during exceptionally big floods since the Red River dike is built by using soil based on a weak foundation of the river delta. According to the Dike Management and Flood Control Bureau of the Ministry of Agriculture and Rural Development of Vietnam, during the 20th century, there have been 20 major breaches in this dike system (Tinh, 2001). In 1971, a historic flood with the return period of 150 years, occurred in the Red River system and caused a real danger of a dike break at Hanoi (Fig.38 and Fig.39). The government had to use some upstream flood diversion areas to protect Hanoi.

4.2 Numerical simulation

The mathematical model was applied in three cases of analysis: (1) a verification analysis for the flood inundation caused by the real heavy rainfall on August 3rd 2001 in the Hanoi area, (2) a simulation of an assumed inundation flood caused by the extraordinarily heavy rainfall of the Nagoya city, Japan (Fig.30), (3) a simulation of a supposed inundation flood caused by an assumed dike break during the historic flood in Hanoi in 1971.

The study area is divided into 5060 unstructured meshes including three categories: the street meshes, the lake and small river meshes and the residence meshes (Fig.25). Small river, lake and street meshes are treated as meshes with lower ground elevation because there is no bank along rivers in the city.

Fig.25 The computation meshes of the study area

The roughness coefficient for street, small river and lake and residence meshes are 0.043, 0.020 and 0.067, respectively. As for drainage capacity or q_{drain}, at present, the drainage and sewerage system of the city is assumed to have capability to decrease 0.01m water per hour. Therefore in computations, q_{drain} at meshes with water depth $h>0.0$ is set to 0.01m/hr, otherwise it is set to zero.

Boundary sections are shown in Fig.26: B1~B2 is high wall boundary; B2~B3 is free overland flow boundary; B3~B1 is high wall boundary including boundary of assumed dike break point.

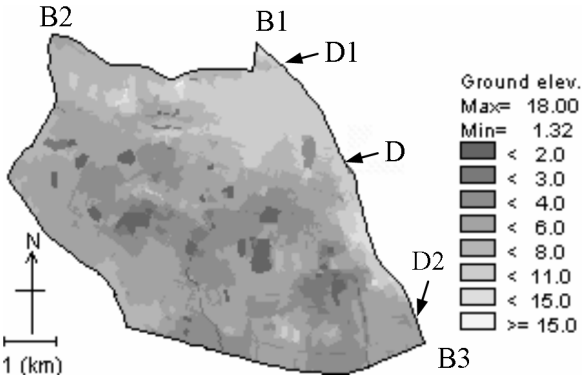

Fig.26 The ground elevation of the study area (D, D1, D2: assumed dike break positions)

(1) Verification analysis using real heavy rainfall data

The rainfall intensity in this analysis is the recorded historic rainfall (0:00 a.m. to 6:00 a.m. supposedly) on August 3rd 2001 in the Hanoi area (Fig.27).

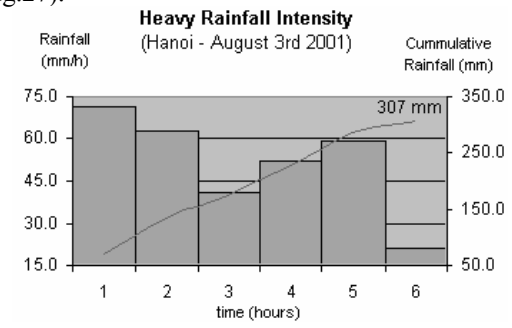

Fig.27 The recorded rainfall

According to the Hanoi Department of Hydrology and Meteorology, the information of some seriously flooded areas caused by this rainfall are shown in Table 1 and Fig.28. The observed data were taken at 9:00 a.m. on August 3rd.

Table 1 Observed water depth (averaged in each area)

Areas (streets)	Water depth
A (Ba Trieu, Nguyen Du…)	about 1.0 m
B (Nguyen Khuyen, Quoc Tu Giam…)	about 0.6 m
C (Nguyen Chi Thanh)	about 0.3 m

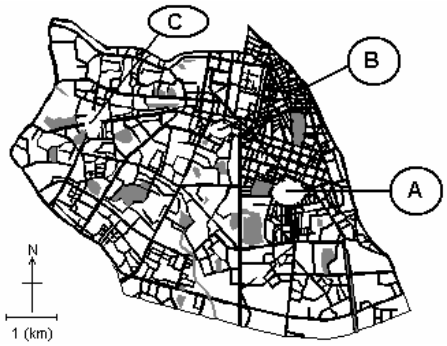

Fig.28 Locations of some seriously flooded areas caused by the heavy rainfall on August 3rd 2001

As shown in Fig.29, computed water depths at places A, B, C at 9:00 a.m. agree quite well with the observed one. However, water depth at place C is a little bit smaller than the observed one. The maximum value at that place during the rain is even smaller than 0.3 m. This could be due to the interpolation of ground elevation because the elevation map used does not have high resolution.

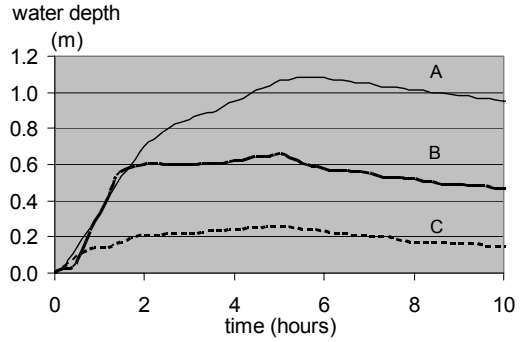

Fig.29 Computed water depth at places A, B, C

(2) Assumed exceptionally heavy rainfall analysis

The observed rainfall intensity of the exceptionally heavy rainfall at the Nagoya city, Japan, is used (Fig.30).

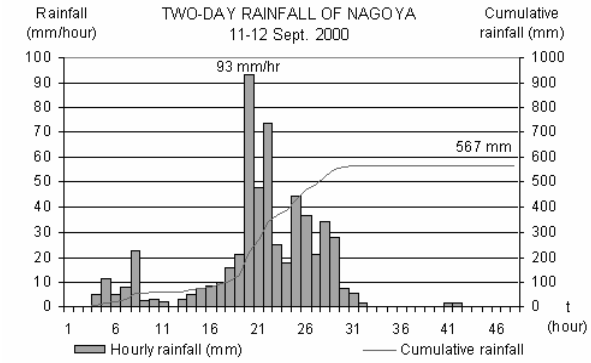

Fig.30 An exceptionally heavy rainfall at Nagoya

The computed results are shown in from Fig.31 to Fig.36. The rain is assumed to start at 0:00 a.m. After 8 hours, some areas, not including lake and small river, are flooded with approximate 0.6 m water depth (Fig.31).

Fig.31 The inundation water depth after 8 hours

Fig.32 The discharge flux after 8 hours

As shown in Fig.33 and Fig.34, after 22 hours, the water depth reaches its peak value of 1.5 m in some areas (except lake and small rivers). This peak value remains for about one hour. As shown in Fig.33, fortunately, almost all the government offices and traditional areas are still safe. In most of these areas, water depth is less than 0.2 m.

Fig.33 The inundation water depth after 22 hours

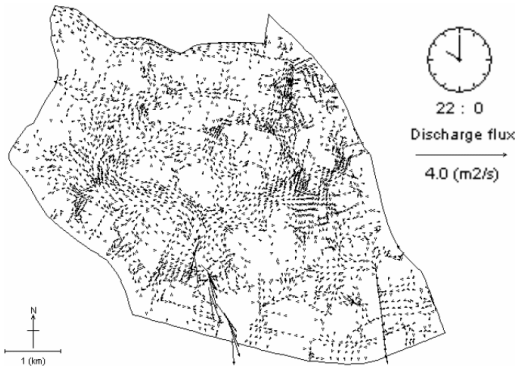

Fig.34 The discharge flux after 22 hours

Fig.35 and Fig.36 show the inundation process after 35 hours. Water depth is still decreasing but very slowly because the present city drainage and sewerage system is not good. The drainage capacity is supposed to be 0.01 m/hr. At that time, the flooded area is no longer too large but the water depth is still high in some low areas. Therefore, measures to evacuate water from low land areas are strongly needed.

Fig.35 The inundation water depth after 35 hours

Fig.36 The discharge flux after 35 hours

As shown in Fig.37, the maximum flooded area with 0.5 m or higher water depth is 18.0 % of the whole study area. After 48 hours, it still remains large, nearly 10 %. It is obvious that the city sewerage and drainage system must be much more improved to cope with such heavy rainfall.

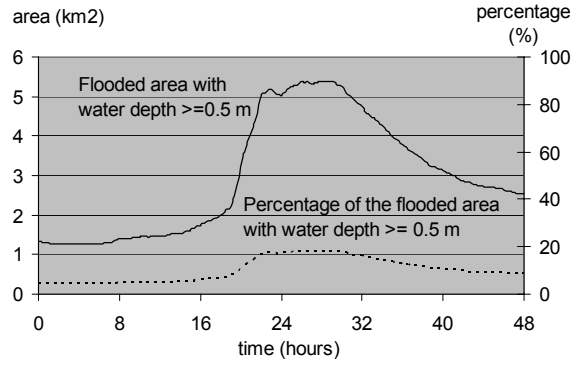

Fig.37 Flooded area with 0.5 m or higher water depth

and its percentage in the whole study area

(3) Assumed dike break analysis

Fig.38 shows the hydrograph observed at Hanoi during the historic flood in August 1971. The real trend of discharge would look like the dotted line which is extrapolated from the observed data, because, at that time, flood water was diverted into the upstream diversion areas to protect Hanoi.

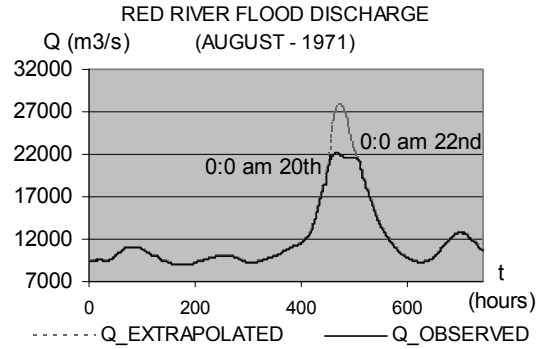

Fig.38 The observed and the extrapolated hydrographs

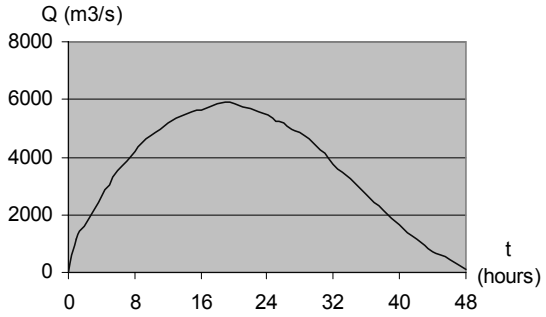

Fig.39 The discharge hydrograph of supposed dike break

The difference between the extrapolated and the observed discharge is adopted into the model as the assumed dike break discharge (Fig.39).

The dike breaks are assumed at three points having lowest ground elevation along Red River dike: D, D1 and D2 (Fig.26).

Computed result for the assumed dike break at point D is shown below. Fig.40 and Fig.41 show the inundation process when the maximum of flood water depth in the area reaches its peak value after 18 hours. In Fig.40, most of the central area is severely flooded with higher than 1.0 m water depth. The major areas, as shown in Fig.22, are also in very dangerous situation.

Fig.40 The maximum water depth after 18 hours

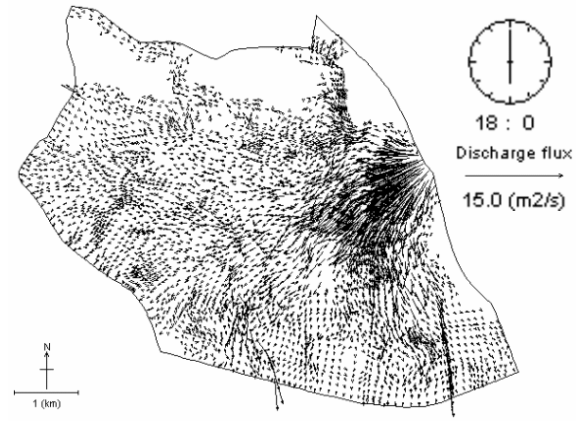

Fig.41 The discharge flux after 18 hours

Fig.42 and Fig.43 show the flood process after 60 hours. At that time the typical water depth, not including river and lake, is about 0.5 m. It means that half a day since water from the dike break stops invading into the area (or two and a half days since the bank break starts), the recovery work could be started.

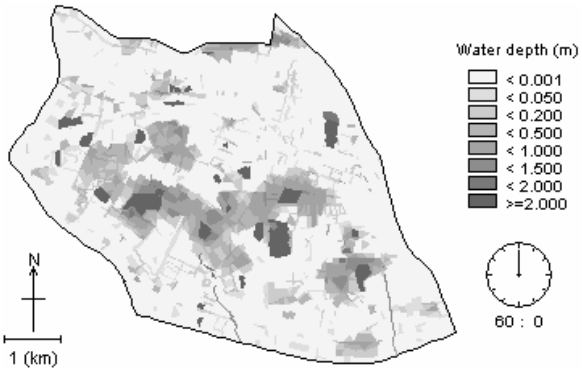

Fig.42 The inundation water depth after 60 hours

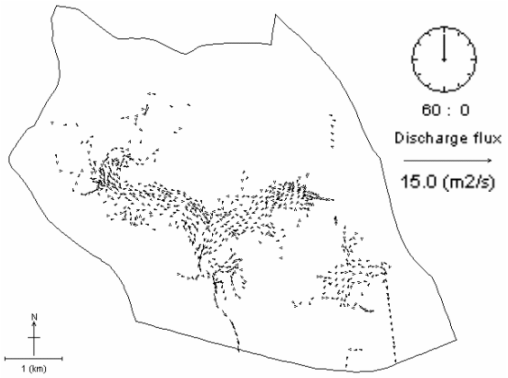

Fig.43 The discharge flux after 60 hours

Fig.44 shows the percentages of flooded area with 0.5 m or higher water depth for three cases. The danger level increases if dike break occurs at more upstream points. The maximum percentages of flooded area of three cases of D, D1 and D2 break points are 76.5%, 89.7% and 68.7 %, respectively.

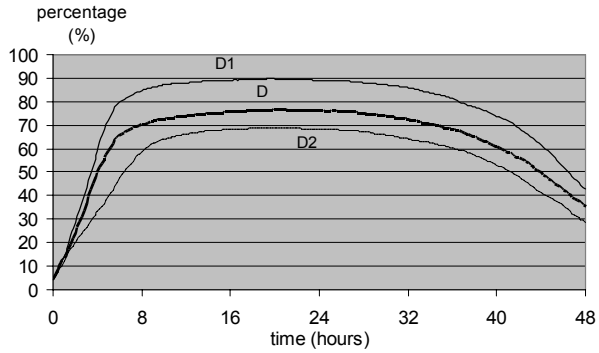

Fig.44 The percentages of flooded area with 0.5 m or greater water depth of three cases of positions of assumed dike break

5. Conclusions and remarks

The model was successfully developed. The verification results are acceptable although some details problems should be much further considered. The result of an assumed heavy rainfall and an assumed dike break analysis give a useful overview of the inundation process of floods if they happen to the city. The model could be a useful tool for the city flood control and for the prediction of inundation process in any flood diversion areas. However, to get better result for city areas, it is necessary to incorporate full drainage systems into the model.

Acknowledgement

The authors are truly grateful to these graduate students: Tokunaga, T., Sagara, R., Nakai, T., Oyagi, R., Nishikori, T., at the Civil Engineering Department, Kyoto University, Japan for their very useful helps to complete the research works and to Mr. Nakagawa, Y., in the same Laboratory for his proof reading of the paper.

References

Kawaike, K., Inoue, K. and Toda, K. (2000): Inundation flow modeling in urban area based on the unstructured meshes, Hydrosoft 2000, Hydraulic Engineering Software, VIII, WIT Press, pp.457-466.

Ishigaki, T., Toda, K. and Inoue, K. (2003): Hydraulic model tests of inundation in urban area with underground space, 30th IAHR Congress, August 2003, Greece, Theme B, pp.487-493.

Iwasa, Y. and Inoue, K. (1982): Mathematical simulation of channel and overland flood flows in view of flood disaster engineering, Journal of Natural Disaster Science, Vol.4, No.1, pp.1-30.

Inoue, K., Nakagawa, H. and Toda, K. (1994): Numerical analysis of overland flood flows by means of one- and two- dimensional models, The 5th JSPS-VCC Seminar On Integrated Engineering, "Engineering Achievement and Challenges", pp.388-397.

Tinh, D. Q. (2001): Participatory planning and management for flood mitigation and preparedness and trends in the Red River basin, Vietnam, Workshop on strengthening capacity in participatory planning and management for flood mitigation and preparedness in large river basins, United Nations Conference center, Bangkok, 20-23 November.

Reference data from Internet websites: www.vnexpress.net on August 5th, 2001 and www.catholic.org.tw.

都市域の洪水氾濫解析モデル：検証と適用

グエン・タット・タン*・井上和也・戸田圭一・川池健司**

*京都大学工学部研究留学生
**長崎大学工学部

要旨

非構造格子に基づく都市域の平面 2 次元氾濫解析モデルが提示されている。解析モデルは京都市街地模型による水理実験結果，ならびにベトナム国ハノイ市の 2001 年の豪雨による内水氾濫の実績値との比較によりその妥当性が確認されている。次にこのモデルを用いて，ハノイ市の 2000 年の東海豪雨に相当する大雨による内水氾濫，紅河の破堤による外水氾濫の解析を実施し，ハノイ市中心部の洪水氾濫時の危険性を議論している。また，モデルは，ハノイ市の治水計画を考えていく上で有用なツールになり得るものである。

キーワード：非構造格子，氾濫解析，モデルの検証，ハノイ，豪雨，破堤，紅河